Euro. Jnl of Applied Mathematics (2002), *vol.* 13, *pp.* 109–128. © 2002 Cambridge University Press
DOI: 10.1017/S0956792501004703 Printed in the United Kingdom

Vibrations of multi-structures including elastic shells: Asymptotic analysis

A. G. ASLANYAN, A. B. MOVCHAN and Ö. SELSIL

Department of Mathematical Sciences, University of Liverpool, Liverpool L69 3BX, UK

(*Received 6 November 2000; revised 6 June 2001*)

We consider an eigenvalue problem of three-dimensional elasticity for a multi-structure consisting of a finite three-dimensional solid linked with a thin-walled elastic cylinder. An asymptotic method is used to derive the junction conditions and to obtain the skeleton model for the multi-structure. Explicit asymptotic formulae have been obtained for the first six eigen-frequencies.

1 Introduction

The asymptotic theory of elastic multi-structures was intensively developed by many researchers during last two decades. The problem of modelling the junctions between bodies of different limit dimensions was explicitly formulated by Ciarlet & Destuynder (1979). The comprehensive monograph by Ciarlet (1997) includes a wide range of asymptotic problems for multi-structures studied by a variational method. An alternative approach, based on the method of compound asymptotic expansions, was developed by Kozlov, Maz'ya & Movchan (1994, 1995, 1996, 1999). Boundary value problems for the Laplacian in 2D–3D multi-structures were studied in Åslund (1998). Justification of theories of elastic shells, based on a variational approach, was published by Berdichevski (1983), Ciarlet & Lods (1996a, 1996b) and Ciarlet, Lods & Miara (1996); spectral analysis for shell structures was presented by Aslanyan & Lidskii (1974), Gol'denveiser, Lidskii & Tovstik (1979), Kesavan & Sabu (2000).

The problem of asymptotic modelling of an elastic multi-structure involving a shell connected to a three-dimensional solid has attracted the attention of researchers for many years and is still a challenge. In the present paper, we study this new problem of vibrations of a multi-structure involving three-dimensional and two-dimensional limit elements (see Figure 1). The elastic fields in the thin cylindrical foundation are described by the equations studied in Aslanyan, Movchan & Selsil (2000).

The paper has the following structure:

- § 2 contains the governing equations and the list of model problems.
- A summary for a lower-dimensional model for a thin-walled cylindrical foundation is given in § 3.

https://doi.org/10.1017/S0956792501004703 Published online by Cambridge University Press

- An algebraic model for a skeleton of the multi-structure is discussed in §4. The frequencies of vibration have been evaluated for two axi-symmetric modes (torsional and longitudinal modes with respect to the $z-$axis).
- In §5, we consider a generalisation for the case of non-axisymmetric vibrations and evaluate the corresponding eigen-frequencies.
- The concluding section includes some examples for a long body on a cylindrical foundation (Sydney centerpoint tower, Liverpool radio tower and a model of a rotten telegraph pole).
- Analysis of the junction conditions and the boundary layer problems are included in the Appendix.

The asymptotic formulae produce numerical values consistent with sample computations, based on the finite element method; the asymptotic formulae are explicit and provide a good approximation for the first eigen-frequencies of the multi-structure.

2 Problem formulation

Let Ω be a three-dimensional finite solid with Lipschitz boundary. Assume that it is supported by a vertical circular hollow cylinder Π_ε of thickness h (see Figure 1). The system of coordinates (x, y, z) is introduced as shown in Figure 1, with the $z-$axis being the axis of the cylinder Π_ε; the centre of mass of the body Ω lies on the $z-$axis, i.e.

$$\int_\Omega x d\mathbf{x} = \int_\Omega y d\mathbf{x} = 0.$$

It is assumed that $2\varepsilon = h/R$ is a small non-dimensional parameter ($0 < \varepsilon \ll 1$); R is the radius of the neutral surface of the cylinder, and l is its height. For the sake of simplicity, we assume that the part of the boundary $\partial\Omega$, connected to Π_ε, is flat and horizontal. We shall use the notation

$$\bar{\Omega}_\varepsilon = \bar{\Omega} \cup \bar{\Pi}_\varepsilon. \tag{2.1}$$

The displacement field $\mathbf{u}$ for small oscillations and the radian frequency ω satisfy the following eigenvalue problem:

$$\mathbf{Lu} + \rho\omega^2\mathbf{u} = \mathbf{0} \quad \text{in} \quad \Omega_\varepsilon, \tag{2.2}$$

$$\boldsymbol{\sigma}^{(\mathbf{n})}(\mathbf{u}) = \mathbf{0} \quad \text{on} \quad \partial\Omega_\varepsilon \setminus S_\varepsilon, \tag{2.3}$$

$$\mathbf{u} = \mathbf{0} \quad \text{on} \quad S_\varepsilon, \tag{2.4}$$

where S_ε denotes the bottom part of the cylinder Π_ε. Here, $\mathbf{L}$ and $\boldsymbol{\sigma}^{(\mathbf{n})}$ stand for the Lamé operator and the operator of tractions. They are defined by the formulae

$$\mathbf{Lu} := \mu\nabla^2\mathbf{u} + (\lambda + \mu)\nabla\nabla \cdot \mathbf{u},$$

and

$$\boldsymbol{\sigma}^{(\mathbf{n})}(\mathbf{u}) = \sigma\mathbf{n},$$

where λ, μ and ρ are the elastic moduli and the material density, respectively; σ is the stress tensor and $\mathbf{n}$ is the unit outward normal on $\partial\Omega_\varepsilon \setminus S_\varepsilon$. The objective of this work is to construct estimates for the lowest eigenvalues of the problem (2.2)–(2.4).

https://doi.org/10.1017/S0956792501004703 Published online by Cambridge University Press

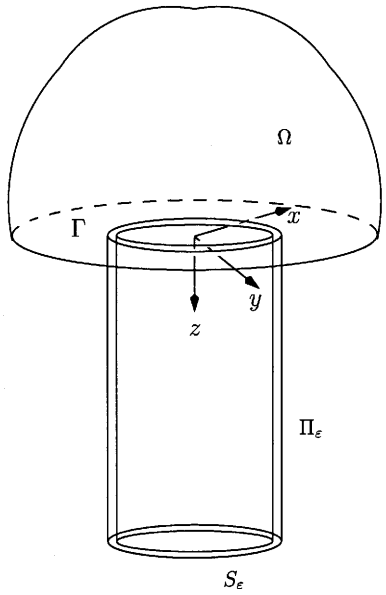


FIGURE 1. The multi-structure.

2.1 Model problems

In general, the asymptotic algorithm involves several model formulations independent of the small parameter:

(1) A problem for the three-dimensional solid Ω.

(2) A lower-dimensional model for the thin-walled cylinder Π_ε; it will be shown that it corresponds to the membrane theory of thin elastic shells.

(3) A boundary layer problem associated with the junction of Π_ε and Ω.

(4) A boundary layer problem corresponding to the base region of Π_ε.

(5) A problem for the limit set a union of a three-dimensional domain and a cylindrical surface which involves evaluation of rigid-body translations and rotations of Ω, and reaction forces and moments at the junction region.

We consider in detail Problems 2 and 5, and give the mathematical formulation and the properties of the solutions for Problems 1 and 3. In our case, the bottom layer (Problem 4) has exponentially small effect far away from the end region and is not considered in the present paper.

3 Derivation of the lower-dimensional model for the thin-walled cylinder Π_ε

We consider the system (2.2) in Π_ε, and assume that interior and exterior cylindrical surfaces are free of tractions, i.e. the boundary condition (2.3) holds on these surfaces. Here, we present a summary of analysis for a cylindrical shell. The detailed study for a shell of general geometry has been included in Aslanyan, Movchan & Selsil (2000). It is convenient to use the cylindrical system of coordinates (r, φ, z), and to introduce a scaled

https://doi.org/10.1017/S0956792501004703 Published online by Cambridge University Press

radial variable

$$\zeta = \frac{r-R}{R\varepsilon}, \quad -1 < \zeta < 1. \tag{3.1}$$

The displacement field is represented in cylindrical coordinates as

$$\mathbf{u} = u_r \mathbf{e}_r + u_\varphi \mathbf{e}_\varphi + u_z \mathbf{e}_z. \tag{3.2}$$

The operators $\mathbf{L}$ and $\boldsymbol{\sigma}^{(\mathbf{n})}$ have the form

$$\mathbf{L}\Big(\frac{\partial}{\partial\zeta}, \frac{\partial}{\partial\varphi}, \frac{\partial}{\partial z}\Big) = \varepsilon^{-2}R^{-2}\mathbf{Q}\frac{\partial^2}{\partial\zeta^2} + \varepsilon^{-1}R^{-1}\mathbf{L}_1\Big(\frac{\partial}{\partial\varphi}, \frac{\partial}{\partial z}\Big)\frac{\partial}{\partial\zeta} + \mathbf{L}_2\Big(\frac{\partial}{\partial\varphi}, \frac{\partial}{\partial z}\Big),$$
$$\boldsymbol{\sigma}^{(\mathbf{n})}\Big(\frac{\partial}{\partial\zeta}, \frac{\partial}{\partial\varphi}, \frac{\partial}{\partial z}; \mathbf{n}\Big) = \varepsilon^{-1}R^{-1}\mathbf{Q}\frac{\partial}{\partial\zeta} + \mathbf{T}_1\Big(\frac{\partial}{\partial\varphi}, \frac{\partial}{\partial z}\Big),$$

where

$$\mathbf{Q} = diag\{\lambda + 2\mu, \mu, \mu\}, \tag{3.3}$$

and the operators $\mathbf{L}_1, \mathbf{L}_2$ and $\mathbf{T}_1$ are the same as in Aslanyan, Movchan & Selsil (2000).

The leading ansatz of the displacement is given by

$$\mathbf{u} \sim \mathbf{u}^{(0)}(\varphi, z) + \varepsilon\mathbf{u}^{(1)}(\zeta, \varphi, z) + \varepsilon^2\mathbf{U}(\zeta, \varphi, z). \tag{3.4}$$

The principal parts of u_r, u_φ and u_z do not depend upon ζ, and they satisfy the following equations (derived as solvability conditions of certain model problems for the components of $\mathbf{U}$):

$$\frac{\partial^2 u_z^{(0)}}{\partial z^2} + \frac{1-\nu}{2R^2}\frac{\partial^2 u_z^{(0)}}{\partial\varphi^2} + \frac{1+\nu}{2R}\frac{\partial^2 u_\varphi^{(0)}}{\partial\varphi\partial z} + \frac{\nu}{R}\frac{\partial u_r^{(0)}}{\partial z} = -\Lambda u_z^{(0)}, \tag{3.5}$$

$$\frac{1-\nu}{2}\frac{\partial^2 u_\varphi^{(0)}}{\partial z^2} + \frac{1}{R^2}\frac{\partial^2 u_\varphi^{(0)}}{\partial\varphi^2} + \frac{1+\nu}{2R}\frac{\partial^2 u_z^{(0)}}{\partial\varphi\partial z} + \frac{1}{R^2}\frac{\partial u_r^{(0)}}{\partial\varphi} = -\Lambda u_\varphi^{(0)}, \tag{3.6}$$

$$\frac{1}{R^2}u_r^{(0)} + \frac{\nu}{R}\frac{\partial u_z^{(0)}}{\partial z} + \frac{1}{R^2}\frac{\partial u_\varphi^{(0)}}{\partial\varphi} = \Lambda u_r^{(0)}, \tag{3.7}$$

where

$$\Lambda = \rho\omega^2\frac{1-\nu^2}{E}, \tag{3.8}$$

and E, ν are the Young modulus and the Poisson ratio, respectively. In particular, for axi-symmetric vibrations

$$u_r^{(0)} = u_r^{(0)}(z), \quad u_\varphi^{(0)} = u_\varphi^{(0)}(z), \quad u_z^{(0)} = u_z^{(0)}(z),$$

and the system (3.5)–(3.7) decouples in the form

$$\frac{d^2 u_z^{(0)}}{dz^2} + \frac{\nu}{R}\frac{du_r^{(0)}}{dz} = -\Lambda u_z^{(0)}, \tag{3.9}$$

$$\frac{d^2 u_\varphi^{(0)}}{dz^2} + \frac{2\Lambda}{1-\nu}u_\varphi^{(0)} = 0, \tag{3.10}$$

$$\frac{\nu}{R}\frac{du_z^{(0)}}{dz} + \Big(\frac{1}{R^2} - \Lambda\Big)u_r^{(0)} = 0. \tag{3.11}$$

https://doi.org/10.1017/S0956792501004703 Published online by Cambridge University Press

4 Skeleton of the multi-structure: axi-symmetric case

4.1 Displacements and forces

First, we shall analyse an axi-symmetric problem.

The skeleton is modelled as a rigid-body solid Ω supported by an elastic cylindrical shell described by equations (3.9)–(3.11). In addition, it is assumed that the base region of the shell is fixed, i.e.

$$u_z^{(0)}(l) = u_\varphi^{(0)}(l) = 0, \tag{4.1}$$

and that the following junction conditions at $z = 0$ hold:

$$u_z^{(0)}(0) = \alpha_3, \quad u_\varphi^{(0)}(0) = \beta_3 R, \tag{4.2}$$

(the Appendix includes the structure of the boundary layer field). The quantities α_3 and β_3 in (4.2) denote the vertical displacement and the angle of torsion for the solid Ω:

$$\mathbf{u} \sim \alpha_3 \mathbf{e}^{(z)} + \beta_3 \mathbf{e}^{(z)} \times \mathbf{x} \quad \text{in} \quad \Omega. \tag{4.3}$$

It follows from (3.9), (3.11) that the function $u_z^{(0)}$ satisfies the following differential equation:

$$\frac{d^2 u_z^{(0)}}{dz^2} + \frac{\Lambda - \dfrac{1}{R^2}}{\Lambda - \left(\dfrac{1-\nu^2}{R^2}\right)} \Lambda u_z^{(0)} = 0. \tag{4.4}$$

The functions $u_z^{(0)}$ and $u_\varphi^{(0)}$ can now be determined as solutions of the boundary value problems (4.4), (3.10), (4.1), (4.2). Then the function $u_r^{(0)}$ can be determined from (3.11). The result is given as follows:

$$u_z^{(0)}(z) = \alpha_3 \{\cos(pz) - \cot(pl)\sin(pz)\}, \tag{4.5}$$

$$u_r^{(0)}(z) = \frac{\nu}{R} \frac{1}{\left(\dfrac{1}{R^2} - \Lambda\right)} p \; \alpha_3 \{\sin(pz) + \cot(pl)\cos(pz)\} \tag{4.6}$$

and

$$u_\varphi^{(0)}(z) = \beta_3 R \{\cos(qz) - \cot(ql)\sin(qz)\}, \tag{4.7}$$

where

$$p = \left(\frac{\Lambda\left(\Lambda - \dfrac{1}{R^2}\right)}{\Lambda - \left(\dfrac{1-\nu^2}{R^2}\right)} \right)^{1/2}, \quad q = \left(\frac{2\Lambda}{1-\nu}\right)^{1/2}. \tag{4.8}$$

We seek values of Λ such that

$$0 < \Lambda < \frac{1-\nu^2}{R^2} \;\Leftrightarrow\; 0 < \frac{\rho\omega^2 R^2}{E} < 1$$

hold, so that p and q are positive.

https://doi.org/10.1017/S0956792501004703 Published online by Cambridge University Press

The reaction force (in the $\mathbf{e}^{(z)}$-direction), exerted by the shell on the body Ω, is given by

$$\begin{aligned}\mathbf{F}_z &= \frac{2\varepsilon ER}{1-\nu^2}\left((u_z^{(0)})' + \nu\frac{u_r^{(0)}}{R}\right)\Big|_{z=0}\mathbf{e}^{(z)} \\ &= -\alpha_3\varepsilon\Xi_1(E,\varepsilon,R,\nu,\Lambda)\mathbf{e}^{(z)}\end{aligned} \tag{4.9}$$

where

$$\Xi_1 = \frac{2ER}{1-\nu^2}\frac{\Lambda - \dfrac{1-\nu^2}{R^2}}{\Lambda - \dfrac{1}{R^2}}\; p\;\cot(pl); \tag{4.10}$$

formulae (4.9), (4.11) are derived in the Appendix, which is related to the analysis of the boundary layer; these formulae are consistent with those in the engineering literature (see, for example, Donnell (1976)).

The tangential reaction force has the form

$$\begin{aligned}\mathbf{F}_\varphi &= \frac{1-\nu}{2}\frac{2\varepsilon ER}{1-\nu^2}(u_\varphi^{(0)})'(0)\mathbf{e}^{(\varphi)} \\ &= -\beta_3\varepsilon\Xi_2(E,\varepsilon,R,\nu,\Lambda)\mathbf{e}^{(\varphi)},\end{aligned} \tag{4.11}$$

where

$$\Xi_2 = \frac{ER^2}{1+\nu}q\;\cot(ql). \tag{4.12}$$

4.2 Eigen-frequencies

To evaluate the first eigen-frequencies for the axi-symmetric multi-structure, subjected to torsional and longitudinal vibrations, we need the following model problems:

$$-\mathbf{L}\mathbf{u}^{(j)} = \boldsymbol{\Psi}^{(j)} \quad \text{in} \quad \Omega, \quad j = 1,2, \tag{4.13}$$

$$\begin{aligned}\boldsymbol{\sigma}^{(\mathbf{n})}(\mathbf{u}^{(j)}) &= \mathbf{F}^{(j)} \\ &= \left(F_z^{(j)}\mathbf{e}^{(z)} + F_\varphi^{(j)}\mathbf{e}^{(\varphi)}\right)\delta(\mathbf{x}-\mathbf{x}^{(0)}), \quad \mathbf{x}\in\partial\Omega,\ \mathbf{x}^{(0)}\in\Gamma,\end{aligned} \tag{4.14}$$

where Γ is the junction contour, and

$$\boldsymbol{\Psi}^{(1)} = \varepsilon\ \mathbf{e}^{(z)}\times\mathbf{x}, \quad \boldsymbol{\Psi}^{(2)} = \varepsilon\ \mathbf{e}^{(z)}. \tag{4.15}$$

We note that $F_z^{(1)} = F_\varphi^{(2)} = 0$, and $F_z^{(2)}, F_\varphi^{(1)}$ have the form (4.9), (4.11), respectively, and depend on the constants α_3, β_3 associated with the rigid-body displacements of the body Ω. In order to find the unknown constants α_3 and β_3 we use the equilibrium equations

$$\int_\Omega \boldsymbol{\Psi}^{(j)}d\mathbf{x} + \int_{\partial\Omega}\mathbf{F}^{(j)}ds = 0, \tag{4.16}$$

$$\int_\Omega \mathbf{x}\times\boldsymbol{\Psi}^{(j)}d\mathbf{x} + \int_{\partial\Omega}\mathbf{x}\times\mathbf{F}^{(j)}ds = 0. \tag{4.17}$$

Within the 3-dimensional body Ω, outside a neighbourhood of the junction contour Γ, the fields $\mathbf{u}^{(j)}$ have the following asymptotics (compare with (4.3))

$$\mathbf{u}^{(1)} \sim \beta_3\mathbf{e}^{(z)}\times\mathbf{x} + O(\varepsilon), \tag{4.18}$$

$$\mathbf{u}^{(2)} \sim \alpha_3\mathbf{e}^{(z)} + O(\varepsilon). \tag{4.19}$$

https://doi.org/10.1017/S0956792501004703 Published online by Cambridge University Press

We note that for $j = 1$ we have $\alpha_3^{(1)} = 0,\ \beta_3^{(1)} = \beta$, and for $j = 2$ the constants are $\alpha_3^{(2)} = \alpha,\ \beta_3^{(2)} = 0$. The constants α, β are determined from (4.16), (4.17), as follows

$$\alpha = \frac{\text{Volume}(\Omega)}{2\pi R \Xi_1}, \quad \beta = \frac{I_3}{2\pi R^2 \Xi_2}, \tag{4.20}$$

where $I_3 = \int_\Omega (x^2 + y^2) d\mathbf{x}$.

The eigenvalues $\omega^{(t)}, \omega^{(l)}$ corresponding to torsional and longitudinal vibrations, are approximated by (it is noted that ω and Λ are related via formula (3.8))

$$\rho\omega^{(t)2} = \frac{\int_\Omega \mathbf{u}^{(1)} \cdot \boldsymbol{\Psi}^{(1)} d\mathbf{x}}{\int_\Omega |\mathbf{u}^{(1)}|^2 d\mathbf{x}} \cong \frac{\varepsilon}{\beta} = \frac{2\pi R^2 \Xi_2(\omega^{(t)})}{I_3}\ \varepsilon, \tag{4.21}$$

for the torsional mode, and

$$\rho\omega^{(l)2} = \frac{\int_\Omega \mathbf{u}^{(2)} \cdot \boldsymbol{\Psi}^{(2)} d\mathbf{x}}{\int_\Omega |\mathbf{u}^{(2)}|^2 d\mathbf{x}} \cong \frac{\varepsilon}{\alpha} = \frac{2\pi R \Xi_1(\omega^{(l)})}{\text{Volume}(\Omega)}\ \varepsilon, \tag{4.22}$$

for the longitudinal mode.

Taking into account that $\Lambda = O(\varepsilon)$, we can write, in accordance with (4.10), (4.12),

$$\Xi_1 \cong \frac{2ER}{l}, \quad \Xi_2 \cong \frac{ER^2}{(1+\nu)l}. \tag{4.23}$$

Hence, we have derived the following approximations:

$$\frac{\omega^{(t)}}{2\pi} = f^{(t)} \cong \frac{1}{\sqrt{2\pi}} \sqrt{\frac{ER^3}{\rho I_3 (1+\nu)}} \sqrt{\frac{\varepsilon R}{l}}, \tag{4.24}$$

for the torsional mode,

$$\frac{\omega^{(l)}}{2\pi} = f^{(l)} \cong \frac{1}{\sqrt{\pi}} \sqrt{\frac{ER}{\rho\ \text{Volume}(\Omega)}} \sqrt{\frac{\varepsilon R}{l}}, \tag{4.25}$$

for the longitudinal mode. As defined in § 2, $2\varepsilon = h/R$.

4.3 Numerical example

The above asymptotic estimates have been compared with the numerical results (we used the finite element software COSMOS/M). For the sample numerical computations, the body Ω was defined as a circular cylinder of diameter D and height H. The following values of the parameters were used for the numerical tests:

$$h = 1[\text{cm}],\ D = 100[\text{cm}],\ H = 100[\text{cm}],\ \rho = 7.8[\frac{\text{g}}{\text{cm}^3}],$$
$$E = 2.1 \times 10^{12}[\frac{\text{g}}{\text{cm} \cdot \text{sec}^2}],\ \nu = 0.3.$$

We have considered a range of values for R and l; the results for the frequencies $f^{(t)}$ and $f^{(l)}$ have been included in Tables 1 and 2. The corresponding vibration modes are

https://doi.org/10.1017/S0956792501004703 Published online by Cambridge University Press

Table 1. *The frequency $f^{(t)}$ [Hz] corresponding to the torsional vibrations about the z-axis*

	l			
R	100 cm	300 cm	500 cm	
12.5 cm	18.1	10.45	8.1	asymptotics
	16.77	9.7	7.52	COSMOS/M
25 cm	51.21	29.57	22.9	asymptotics
	49.02	28.31	21.88	COSMOS/M

Table 2. *The frequency $f^{(l)}$ [Hz] corresponding to the longitudinal vibrations along the z-axis*

	l			
R	100 cm	300 cm	500 cm	
12.5 cm	82.58	47.68	36.93	asymptotics
	80.29	46.48	35.93	COSMOS/M
25 cm	116.79	67.43	52.23	asymptotics
	114.64	66.10	50.92	COSMOS/M

illustrated in Figures 3(b), 3(d). The asymptotic formulae (4.24), (4.25) give upper bounds for the eigen-frequencies and provide an accurate approximation consistent with the results of sample numerical computations. We note that the finite element computations, with the mesh involving more than 10,000 elements, required more than 90 minutes of processor time on a Pentium II PC. On the other hand, the asymptotic formulae are explicit and provide excellent accuracy.

5 Generalisation to the case of non-axisymmetric vibrations

5.1 Lower dimensional model problems

We consider the same multi-structure Ω_ε, as in §1, and evaluate the frequencies ω in problem (2.2)–(2.4) corresponding to non-axisymmetric vibrations. The vibration modes mentioned are associated with the horizontal translations of Ω and rotations of Ω about horizontal axis.

Let $\mathbf{u}$ solve the auxiliary problem (4.13)–(4.14) with $\boldsymbol{\Psi}$ being defined by

$$\boldsymbol{\Psi} = C_1 b_0 \mathbf{e}^{(2)} \times \mathbf{x} + C_2 b_0 a_0 \mathbf{e}^{(1)}, \tag{5.1}$$

where C_1, C_2 are non-dimensional constant coefficients, and let a_0, b_0 define the physical dimensions, i.e.

$$a_0 = 1[cm] \quad \text{and} \quad b_0 = 1\left[\frac{\mathrm{g}}{\mathrm{cm}^3 \cdot \mathrm{sec}^2}\right].$$

https://doi.org/10.1017/S0956792501004703 Published online by Cambridge University Press

Similar to § 4, in Ω outside Γ the vector $\mathbf{u}$ is sought in the form

$$\mathbf{u} = \beta_2 \mathbf{e}^{(2)} \times \mathbf{x} + \alpha_1 a_0 \mathbf{e}^{(1)} + O(\varepsilon), \tag{5.2}$$

the coefficients β_2, α_1 are non-dimensional. Without loss of generality we consider the translation of Ω along the x_1-axis and the rotation of Ω about the x_2-axis.

The boundary conditions for the functions $u_z^{(0)}$ and $u_\varphi^{(0)}$, associated with the cylindrical shell, are formulated in the form

$$u_z^{(0)}\Big|_{z=0} = -\beta_2 R \cos\varphi, \quad u_\varphi^{(0)}\Big|_{z=0} = -\alpha_1 a_0 \sin\varphi, \tag{5.3}$$

and

$$u_z^{(0)}\Big|_{z=l} = u_\varphi^{(0)}\Big|_{z=l} = 0. \tag{5.4}$$

The functions $u_z^{(0)}, u_\varphi^{(0)}$ corresponding to the leading approximation of the displacement within the thin shell, satisfy the following system of partial differential equations (compare with (3.5)–(3.6)):

$$p_1 \frac{\partial^2 u_z^{(0)}}{\partial z^2} + p_2 \frac{1}{R^2} \frac{\partial^2 u_z^{(0)}}{\partial \varphi^2} + p_3 \frac{1}{R} \frac{\partial^2 u_\varphi^{(0)}}{\partial \varphi \partial z} + \Lambda u_z^{(0)} = 0, \tag{5.5}$$

$$p_2 \frac{\partial^2 u_\varphi^{(0)}}{\partial z^2} + p_4 \frac{1}{R^2} \frac{\partial^2 u_\varphi^{(0)}}{\partial \varphi^2} + p_3 \frac{1}{R} \frac{\partial^2 u_z^{(0)}}{\partial \varphi \partial z} + \Lambda u_\varphi^{(0)} = 0. \tag{5.6}$$

Here, the coefficients are non-dimensional and have the form

$$p_1 = \frac{(1-\nu^2)\kappa^2 - \Lambda}{\kappa^2 - \Lambda}, \; p_2 = \frac{1}{2}(1-\nu), \; p_3 = \frac{1+\nu}{2} - \frac{\nu\kappa^2}{\kappa^2 - \Lambda},$$
$$p_4 = -\frac{\Lambda}{\kappa^2 - \Lambda}, \; \kappa = R^{-1}.$$

The problem (5.5), (5.6), (5.3), (5.4) allows for a solution represented by:

$$\begin{aligned} u_z^{(0)}(\varphi, z) &= -\{\beta_2 R u_1(z, \Lambda) - \alpha_1 a_0 u_2(z, \Lambda)\} \cos\varphi, \\ u_\varphi^{(0)}(\varphi, z) &= -\{\beta_2 R v_1(z, \Lambda) - \alpha_1 a_0 v_2(z, \Lambda)\} \sin\varphi, \end{aligned} \tag{5.7}$$

where the fields (u_j, v_j) are defined as solutions of a system of ordinary differential equations:

$$\begin{aligned} p_1 u_j'' + (\Lambda - p_2\kappa^2) u_j + p_3 \kappa v_j' &= 0, \\ p_2 v_j'' + (\Lambda - p_4\kappa^2) v_j - p_3 \kappa u_j' &= 0, \end{aligned} \tag{5.8}$$

for $0 < z < l, \; j = 1, 2$. The system (5.8) is complemented by the boundary conditions

$$\begin{aligned} u_1\Big|_{z=0} &= 1, \; v_1\Big|_{z=0} = 0, \\ u_1\Big|_{z=l} &= v_1\Big|_{z=l} = 0, \end{aligned} \tag{5.9}$$

and

$$\begin{aligned} u_2\Big|_{z=0} &= 0, \; v_2\Big|_{z=0} = 1, \\ u_2\Big|_{z=l} &= v_2\Big|_{z=l} = 0. \end{aligned} \tag{5.10}$$

https://doi.org/10.1017/S0956792501004703 Published online by Cambridge University Press

5.2 Forces and moments at the junction contour

The thin cylindrical foundation Π_ε exerts the reaction forces on the body Ω (see the Appendix; also see Donnell (1976)), with the following force densities per unit length:

$$F_z^{(0)} = \frac{Eh}{1-\nu^2}\Big(\frac{\partial u_z^{(0)}}{\partial z} + \kappa\nu\frac{\partial u_\varphi^{(0)}}{\partial \varphi} + \kappa\nu u_r^{(0)}\Big)\Big|_{z=0}, \tag{5.11}$$

$$F_\varphi^{(0)} = \frac{Eh}{2(1+\nu)}\Big(\frac{\partial u_\varphi^{(0)}}{\partial z} + \kappa\frac{\partial u_z^{(0)}}{\partial \varphi}\Big)\Big|_{z=0}. \tag{5.12}$$

We note that $F_r^{(0)}$ and all moments have the order $O(\varepsilon^3)$ and they do not contribute to the leading-order approximation of the solution. It is straightforward to verify that the Cartesian components of force densities are given by the formulae:

$$F_1^{(0)} = -\frac{Eh}{2(1+\nu)}\{\beta_2(1 - Rv_1'|_{z=0}) + \alpha_1 a_0 v_2'|_{z=0}\}\ \sin^2\varphi, \tag{5.13}$$

$$F_2^{(0)} = \frac{Eh}{2(1+\nu)}\{\beta_2(1 - Rv_1'|_{z=0}) + \alpha_1 a_0 v_2'|_{z=0}\}\ \sin\varphi\ \cos\varphi, \tag{5.14}$$

$$F_3^{(0)} = -\frac{Eh}{1-\nu^2}\Big\{p_1\big(\beta_2 Ru_1'|_{z=0} - \alpha_1 a_0 u_2'|_{z=0}\big) + \frac{\kappa\nu\Lambda}{\Lambda-\kappa^2}\alpha_1 a_0\Big\}\ \cos\varphi. \tag{5.15}$$

Direct integration with respect to φ shows that the principal components, in the directions of the x_2 and x_3 axes, vanish. On the other hand, the x_1-component of the principal force is given by

$$\begin{aligned}\mathscr{F}_1 &= \int_0^{2\pi} F_1^{(0)} R d\varphi \\ &= -\frac{Eh\pi R}{2(1+\nu)}\{\beta_2(1 - Rv_1'|_{z=0}) + \alpha_1 a_0 v_2'|_{z=0}\}.\end{aligned} \tag{5.16}$$

Next, we evaluate the principal moment of the reaction forces:

$$\begin{aligned}\mathscr{M} &= \int_\Gamma \mathbf{x}\times\mathbf{F}^{(0)} ds \\ &= \frac{Eh\pi R^2}{1-\nu^2}\Big\{p_1\big(\beta_2 Ru_1'|_{z=0} - \alpha_1 a_0 u_2'|_{z=0}\big) + \frac{\kappa\nu\Lambda}{\Lambda-\kappa^2}\alpha_1 a_0\Big\}\mathbf{e}^{(2)}.\end{aligned} \tag{5.17}$$

To evaluate $u_j'|_{z=0}, v_j'|_{z=0}$ we need to solve problems (5.8), (5.9) and (5.8), (5.10). One can also note that the first eigen-frequencies have the order $O(\varepsilon^{1/2})$, and hence $\Lambda = O(\varepsilon)$.

When $\varepsilon \ll 1$, the following approximation can be used:

$$\frac{dv_j}{dz}(0,\Lambda) \cong \frac{dv_j}{dz}(0,0), \quad \frac{du_j}{dz}(0,\Lambda) \cong \frac{du_j}{dz}(0,0). \tag{5.18}$$

The system (5.8), when $\Lambda = 0$, simplifies and can be easily integrated:

$$\begin{aligned}u_1(z,0) &= 1 + d_1 z - \frac{\kappa}{4(1+\nu)}d_2 z^2, \\ v_1(z,0) &= d_2 z + \kappa\Big(z + d_1\frac{z^2}{2} - \frac{\kappa}{12(1+\nu)}d_2 z^3\Big),\end{aligned} \tag{5.19}$$

https://doi.org/10.1017/S0956792501004703 Published online by Cambridge University Press

where

$$d_1 = -\frac{4\kappa^2 l^2 + 24(1+\nu)}{l(\kappa^2 l^2 + 24(1+\nu))}, \quad d_2 = \frac{4(1+\nu)}{\kappa l^2}(d_1 l + 1), \tag{5.20}$$

and

$$\begin{aligned} u_2(z,0) &= \frac{\kappa}{4(1+\nu)} d_3(lz - z^2), \\ v_2(z,0) &= 1 + d_3\Big[z + \frac{\kappa^2}{4(1+\nu)}\Big(\frac{z^2 l}{2} - \frac{z^3}{3}\Big)\Big], \end{aligned} \tag{5.21}$$

where

$$d_3 = -\frac{24(1+\nu)}{l(\kappa^2 l^2 + 24(1+\nu))}. \tag{5.22}$$

Substituting (5.19), (5.21) into (5.16), (5.17), we obtain

$$\mathscr{F}_1 = -\beta_2 \mathscr{F}_{11} + \alpha_1 \mathscr{F}_{12}, \tag{5.23}$$

where

$$\mathscr{F}_{11} = \frac{6\pi REh}{\kappa^2 l^2 + 24(1+\nu)}, \quad \mathscr{F}_{12} = \frac{12\pi REh}{l(\kappa^2 l^2 + 24(1+\nu))} a_0, \tag{5.24}$$

and

$$\mathscr{M} = (\beta_2 \mathscr{M}_1 - \alpha_1 \mathscr{M}_2)\mathbf{e}^{(2)}, \tag{5.25}$$

where

$$\mathscr{M}_1 = \frac{(4\kappa^2 l^2 + 24(1+\nu))\pi R^3 Eh}{l(\kappa^2 l^2 + 24(1+\nu))}, \quad \mathscr{M}_2 = \frac{6\pi REh}{\kappa^2 l^2 + 24(1+\nu)} a_0. \tag{5.26}$$

5.3 Estimates for the eigen-frequencies

The balance of moments (see (4.17)) yields

$$C_1 b_0 I_2 + C_2 b_0 a_0 \kappa_0 = \beta_2 \mathscr{M}_1 - \alpha_1 \mathscr{M}_2. \tag{5.27}$$

Equation (4.16), representing the balance of forces, reduces to the form

$$C_1 b_0 \kappa_0 + C_2 b_0 a_0 \Omega_0 = -\beta_2 \mathscr{F}_{11} + \alpha_1 \mathscr{F}_{12}. \tag{5.28}$$

In system (5.27), (5.28) we have used the following notations:

$$I_2 = \int_\Omega (x^2 + z^2) d\mathbf{x}, \quad \Omega_0 = \text{Volume}(\Omega), \quad \kappa_0 = \int_\Omega z \; d\mathbf{x}.$$

Using the notations

$$\mathbf{C} = (C_1, C_2)^T, \quad \boldsymbol{\gamma} = (\beta_2, \alpha_1)^T$$

we represent the system (5.27), (5.28) in the matrix form

$$\sigma_0 \mathbf{C} = b_0^{-1} \mathscr{A} \boldsymbol{\gamma}, \tag{5.29}$$

where

$$\sigma_0 = \begin{pmatrix} I_2 & a_0 \kappa_0 \\ a_0 \kappa_0 & a_0^2 \Omega_0 \end{pmatrix}, \tag{5.30}$$

https://doi.org/10.1017/S0956792501004703 Published online by Cambridge University Press

$$\mathscr{A} = \begin{pmatrix} \mathscr{M}_1 & -\mathscr{M}_2 \\ -a_0\mathscr{F}_{11} & a_0\mathscr{F}_{12} \end{pmatrix}. \tag{5.31}$$

It follows from (5.24), (5.26) that $\mathscr{M}_2 = a_0\mathscr{F}_{11}$. Correspondingly, both matrices σ_0 and $\mathscr{A}$ are symmetric. The solution of (5.29) is given by

$$\mathbf{C} = b_0^{-1}\sigma_0^{-1}\mathscr{A}\boldsymbol{\gamma}. \tag{5.32}$$

It is noted that by Cauchy inequality, $\det \sigma_0 \neq 0$.

The frequency ω satisfies the inequality (compare with Kozlov, Maz'ya & Movchan (1999))

$$\rho\omega^2 \leqslant t = \min_{\mathbf{u}\neq 0} \frac{\int_\Omega (\mathbf{u}, \boldsymbol{\Psi}) d\mathbf{x}}{\int_\Omega (\mathbf{u}, \mathbf{u}) d\mathbf{x}}. \tag{5.33}$$

Using (5.1), (5.2), (5.32) we derive that

$$t = \min_{|\boldsymbol{\gamma}|=1} \frac{(\boldsymbol{\gamma}, \mathscr{A}\boldsymbol{\gamma})}{(\boldsymbol{\gamma}, \sigma_0\boldsymbol{\gamma})}, \tag{5.34}$$

which represents the corresponding algebraic problem. The quantity t satisfies the following algebraic equation:

$$\det (t\sigma_0 - \mathscr{A}) = 0. \tag{5.35}$$

It is verified directly that this equation has two real positive roots

$$0 < t_1 \leqslant t_2. \tag{5.36}$$

Furthermore, the frequencies $f_1^{(b)}, f_2^{(b)}$ can be approximated[1] by

$$f_j^{(b)} = \frac{\omega_j^{(b)}}{2\pi} \cong \frac{1}{2\pi}\sqrt{\frac{t_j}{\rho}} = \frac{1}{2\pi}\sqrt{\frac{\pi REh}{\kappa^2 l^2 + 24(1+\nu)}}\sqrt{\frac{\eta_j}{\rho}}, \tag{5.37}$$

where η_j, $j = 1, 2$, denote the roots of the quadratic equation

$$s_0\eta^2 - s_1\eta + s_2 = 0, \tag{5.38}$$

$$\begin{aligned} s_0 &= I_2\Omega_0 - \kappa_0^2, \\ s_1 &= 4l\Big(1 + \frac{6(1+\nu)}{\kappa^2 l^2}\Big)\Omega_0 + \frac{12}{l}I_2 + 12\kappa_0, \\ s_2 &= 12 + \frac{288(1+\nu)}{\kappa^2 l^2}. \end{aligned}$$

5.4 Numerical example

We consider the same multi-structure as in § 3.3. In Tables 3 and 4 we give the values of eigen-frequencies $f_1^{(b)}, f_2^{(b)}$ corresponding to non-axisymmetric vibration modes shown in Figures 3(a) and 3(c).

[1] This asymptotic estimate provides an upper bound, and it will be shown that it is in agreement with the results based on the finite element method.

https://doi.org/10.1017/S0956792501004703 Published online by Cambridge University Press

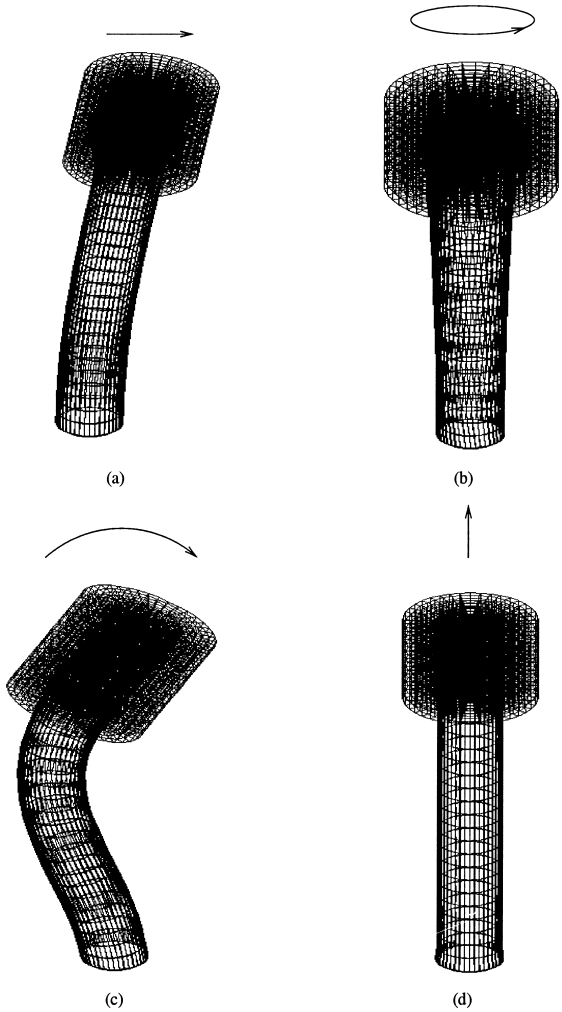


FIGURE 2. Vibration modes of the multi-structure.

Table 3. *The frequency* $f_1^{(b)}$ *[Hz] for the bending-translation mode*

R	l 100 cm	300 cm	500 cm	
12.5 cm	6.51	1.9	0.97	asymptotics
	6.14	1.79	0.92	COSMOS/M
25 cm	17.67	5.31	2.74	asymptotics
	17.18	5.15	2.65	COSMOS/M

https://doi.org/10.1017/S0956792501004703 Published online by Cambridge University Press

Table 4. *The frequency* $f_2^{(b)}$ *[Hz] for the bending-translation mode*

		l			
	R	100 cm	300 cm	500 cm	
	12.5 cm	60.83	27.51	19.67	asymptotics
		56.39	24.74	16.68	COSMOS/M
	25 cm	127.41	73.30	54.38	asymptotics
		121.17	65.82	43.51	COSMOS/M

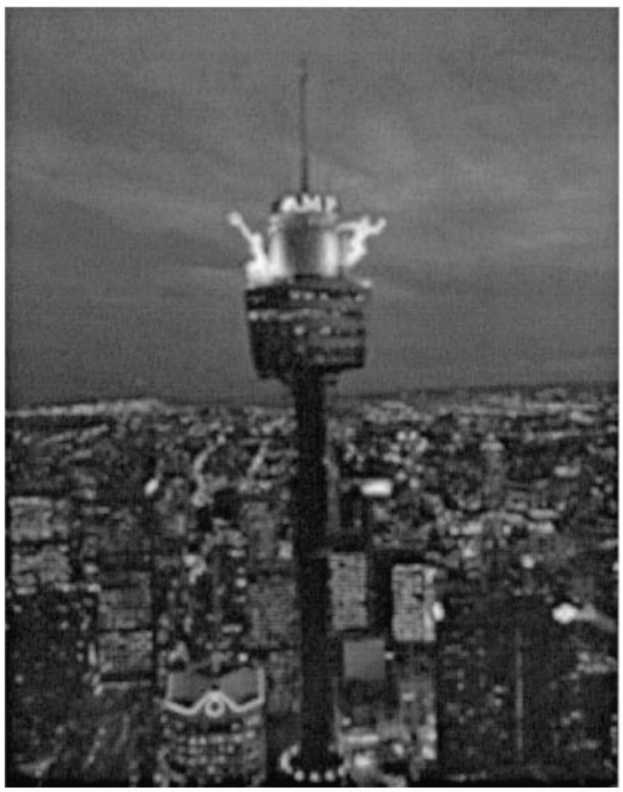


FIGURE 3. Sydney centerpoint tower.

Comparing this case with § 3.3, we note (see formulae (5.30), (5.31)) that the vibration modes, corresponding to 'bending' of the elastic shell, do not decouple. It is evident that the asymptotic formulae (5.37) provide good approximation for the eigen-frequencies $f_j^{(b)}$, $j = 1, 2$.

6 Concluding remarks

(1) First, we note that the right-hand sides of (4.24), (4.25) and (5.37) give the upper bounds for the eigen-frequencies of the multi-structure. Numerical tests

https://doi.org/10.1017/S0956792501004703 Published online by Cambridge University Press

Table 5. *The first frequency* $f_1^{(b)}$ *for a 'rotten telegraph pole'*

h	Asymptotics	COSMOS/M
0.5 cm	3.98 Hz	3.03 Hz
1 cm	5.64 Hz	4.29 Hz

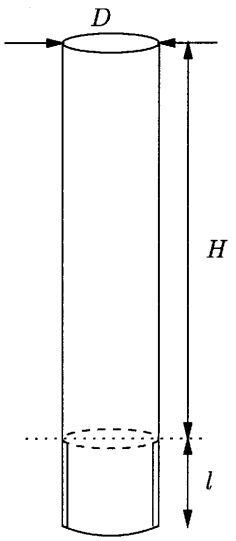


FIGURE 4. A long body on a cylindrical foundation (a rotten telegraph pole).

(see Tables 1–4) show that these upper bounds, constructed in accordance with our asymptotic algorithm, are sufficiently close to the exact values of the eigen-frequencies.

We also note that the first eigen-frequencies have the order $O(\varepsilon^{1/2})$ which are greater compared to the eigen-frequencies for the multi-structures that involve thin rods and three-dimensional bodies (see Kozlov, Maz'ya & Movchan (1999)).

(2) The multi-structure Ω_ε, considered in the present paper, involves several geometrical and physical parameters. The non-dimensional small parameter $\varepsilon = h/2R$ was related to the thickness h and the radius R of the cylindrical support. For the case when the height l is larger than the radius R, our model can be applied, for example, in evaluation of eigenfrequencies of structures like Sydney centerpoint tower (see Figure 3) or Liverpool radio tower. Our asymptotic formulae are still efficient for a wide range of geometrical and physical parameters. Consider, for example, a model of a rotten telegraph pole (see Figure 4), where a long cylindrical body of diameter D and height H stands on a cylindrical foundation of height l, radius R and thickness h. The asymptotic formula (5.37), $j = 1$, gives approximation for the first eigen-frequency associated with the bending-translation mode.

https://doi.org/10.1017/S0956792501004703 Published online by Cambridge University Press

For the sample computations we used the following values of the parameters:

$$2R = D = 25[\text{cm}],\ H = 450[\text{cm}],$$
$$l = 50[\text{cm}],\ E = 1.1 \times 10^{11}\left[\frac{\text{g}}{\text{cm} \cdot \text{sec}^2}\right],$$
$$\rho = 0.61\left[\frac{\text{g}}{\text{cm}^3}\right],\ \nu = 0.3.$$

The asymptotic approximations and the numerical estimates are included in Table 5.

The asymptotic formula (5.37) provides an upper estimate which is consistent with the results of numerical tests based on the finite element method.

(3) In this paper, we have obtained new explicit asymptotic formulae for the eigenfrequencies of a 2D–3D multi-structure. The method of compound asymptotic expansions has been effectively used to derive the junction conditions and the lower-dimensional model of the skeleton of the multi-structure. The asymptotic estimates gave a good agreement with the results of sample finite element computations. The ideas implemented in the present asymptotic algorithm are quite general and can be applied to multi-structures involving thin shells of arbitrary geometry and inhomogeneous multi-structures.

Appendix A: Boundary layers for the axi-symmetric case

A.1 Cut-off functions and local coordinates

Let $\mathbf{x}_0$ be an arbitrary point on Γ. Locally, in a neighbourhood of the junction contour we introduce two smooth cut-off functions χ and Ξ in such a way that

$$\chi\Big(\frac{|\mathbf{x}-\mathbf{x}_0|}{\varepsilon}\Big) = \begin{cases} 1, & \dfrac{|\mathbf{x}-\mathbf{x}_0|}{\varepsilon} > 2, \\ 0, & \dfrac{|\mathbf{x}-\mathbf{x}_0|}{\varepsilon} < 1, \end{cases}$$

and $\chi = 0$ outside Ω, and

$$\Xi\Big(\frac{z}{\varepsilon}\Big) = \begin{cases} 1, & \dfrac{z}{\varepsilon} > 2, \\ 0, & \dfrac{z}{\varepsilon} < 1. \end{cases}$$

It is noted that the cut-off functions χ and Ξ will be used with the fields defined in Ω and Π_ε, respectively.

Local coordinates (n, z, s) are introduced in the vicinity of the junction contour Γ (see Figure 2). The scaled coordinates $\boldsymbol{\xi}$ are defined as follows:

$$(\xi_1, \xi_2, \xi_3) = \Big(\frac{n}{\varepsilon}, \frac{z}{\varepsilon}, s\Big).$$

https://doi.org/10.1017/S0956792501004703 Published online by Cambridge University Press

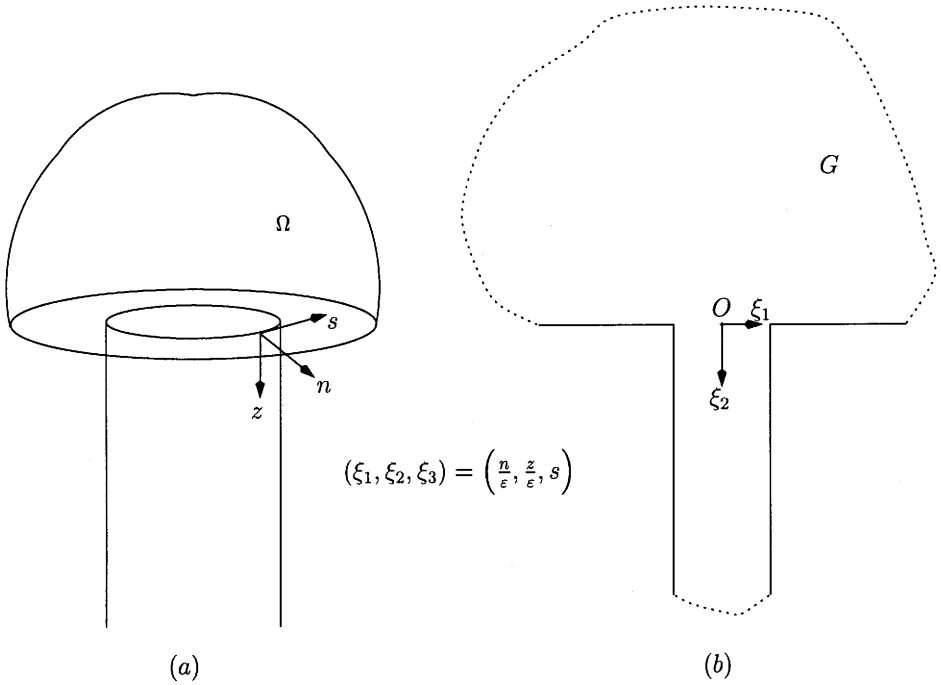


FIGURE 1. (a) Skeleton of the multi-structure; (b) the two-dimensional domain corresponding to the junction layer.

A.2 Expansion of the displacement in the vicinity of the junction region

In this section, we give a sketch of the asymptotic scheme corresponding to the analysis of the boundary layers. We shall need the fields $\mathbf{u}_\Omega$ and $\mathbf{u}_\Pi$ representing the solutions in the region Ω and Π_ε.

Here, $\mathbf{u}_\Omega$ solves a problem of the type (4.13), (4.14) and satisfies the following orthogonality conditions:

$$\int_\Omega \mathbf{u}_\Omega d\mathbf{x} = \mathbf{0}, \quad \int_\Omega \mathbf{x} \times \mathbf{u}_\Omega d\mathbf{x} = \mathbf{0}; \tag{A.1}$$

the field $\mathbf{u}_\Pi$ corresponds to the displacement in Π_ε and has the structure defined by (3.4).

In a neighbourhood of the junction region the displacement field is represented in the form

$$\mathbf{u} \sim \chi \mathbf{u}_\Omega + \Xi \mathbf{u}_\Pi + \mathscr{W}^\frown + (1 - \Xi)\varepsilon^{-1}(\alpha_3 \mathbf{e}^{(z)} + \beta_3 \mathbf{e}^{(z)} \times \mathbf{x}), \tag{A.2}$$

where $\mathscr{W}^\frown$ is the junction layer field which compensates for the discrepancy of $\chi \mathbf{u}_\Omega$ and $\Xi \mathbf{u}_\Pi$ in the governing equations and the boundary conditions.

Similar to Kozlov, Maz'ya & Movchan (1999) and Aslanyan, Movchan & Selsil (2000), the fields $\mathbf{u}_\Omega, \mathbf{u}_\Pi$ can be approximated by

$$\mathbf{u}_\Omega = \mathscr{T} + \mathscr{R}, \tag{A.3}$$

$$\mathbf{u}_\Pi = \varepsilon^{-1}\mathbf{u}^{(0)}(\varphi, z) + \mathbf{u}^{(1)}(\zeta, \varphi, z) + \varepsilon \mathbf{U}(\zeta, \varphi, z), \tag{A.4}$$

https://doi.org/10.1017/S0956792501004703 Published online by Cambridge University Press

where $\mathscr{T}$ is a log-singular vector function, $\mathscr{R}$ is a smooth vector field, and $\mathbf{u}^{(0)}$ satisfies the equations of the membrane shell theory, as derived in (3.9), (3.10) and (3.11). We also note that $u_r^{(0)}|_{z=0} = 0$. The junction layer $\mathscr{W}$ admits the asymptotic approximation

$$\mathscr{W} \sim \varepsilon^{-1}\mathscr{W}^{(0)}(\boldsymbol{\xi}') + \mathscr{W}^{(1)}(\boldsymbol{\xi}', \log\varepsilon) + \text{smaller terms}, \tag{A.5}$$

where $\boldsymbol{\xi}' = (\xi_1, \xi_2)$. As it will be shown below, the $\log\varepsilon$ dependence in $\mathscr{W}^{(1)}$ occurs due to the fact that the function $\mathscr{T}$ in (A.3) is log-singular. The vector functions $\mathscr{W}^{(0)}, \mathscr{W}^{(1)}$ are defined in the scaled two-dimensional region G (see Figure 2(b)), represented as a union of a half-plane and a semi-infinite strip.

We use block-diagonal differential operators defined by

$$\mathscr{L}\Big(\frac{\partial}{\partial\boldsymbol{\xi}'}\Big) = \begin{pmatrix} \mu\nabla^2_{\boldsymbol{\xi}'} + (\lambda+\mu)\dfrac{\partial^2}{\partial\xi_1^2} & (\lambda+\mu)\dfrac{\partial^2}{\partial\xi_1\partial\xi_2} & 0 \\ (\lambda+\mu)\dfrac{\partial^2}{\partial\xi_1\partial\xi_2} & \mu\nabla^2_{\boldsymbol{\xi}'} + (\lambda+\mu)\dfrac{\partial^2}{\partial\xi_2^2} & 0 \\ 0 & 0 & \mu\nabla^2_{\boldsymbol{\xi}'} \end{pmatrix}, \tag{A.6}$$

$$\begin{aligned} \boldsymbol{\Sigma}^{(\mathbf{n})}\Big(\frac{\partial}{\partial\boldsymbol{\xi}'}\Big) = n_1 &\begin{pmatrix} (\lambda+2\mu)\dfrac{\partial}{\partial\xi_1} & \lambda\dfrac{\partial}{\partial\xi_2} & 0 \\ \mu\dfrac{\partial}{\partial\xi_2} & \mu\dfrac{\partial}{\partial\xi_1} & 0 \\ 0 & 0 & \mu\dfrac{\partial}{\partial\xi_1} \end{pmatrix} \\ + n_2 &\begin{pmatrix} \mu\dfrac{\partial}{\partial\xi_2} & \mu\dfrac{\partial}{\partial\xi_1} & 0 \\ \lambda\dfrac{\partial}{\partial\xi_1} & (\lambda+2\mu)\dfrac{\partial}{\partial\xi_2} & 0 \\ 0 & 0 & \mu\dfrac{\partial}{\partial\xi_2} \end{pmatrix}. \end{aligned} \tag{A.7}$$

Direct substitution into the equations and boundary conditions yields

$$\begin{aligned} &\mathscr{L}\Big(\frac{\partial}{\partial\boldsymbol{\xi}'}\Big)\mathscr{W}^{(0)}(\boldsymbol{\xi}') + [\mathscr{L}, \Xi]\big(u_z^{(0)}(\varphi,0)\mathbf{e}^{(z)} \\ &+u_\varphi^{(0)}(\varphi,0)\mathbf{e}^{(\varphi)} - \alpha_3\mathbf{e}^{(z)} - \beta_3\mathbf{e}^{(z)}\times\mathbf{x}_0\big) = 0 \ \text{ in } G, \end{aligned} \tag{A.8}$$

$$\begin{aligned} &\boldsymbol{\Sigma}^{(\mathbf{n})}\Big(\frac{\partial}{\partial\boldsymbol{\xi}'}\Big)\mathscr{W}^{(0)}(\boldsymbol{\xi}') + [\boldsymbol{\Sigma}^{(\mathbf{n})}, \Xi]\big(u_z^{(0)}(\varphi,0)\mathbf{e}^{(z)} \\ &+u_\varphi^{(0)}(\varphi,0)\mathbf{e}^{(\varphi)} - \alpha_3\mathbf{e}^{(z)} - \beta_3\mathbf{e}^{(z)}\times\mathbf{x}_0\big) = 0 \ \text{ on } \partial G. \end{aligned} \tag{A.9}$$

Here, $\mathbf{x}_0$ is a point at the junction contour Γ and $[\mathscr{L}, \Xi] = \mathscr{L}\Xi - \Xi\mathscr{L}$ is the commutator of the operator $\mathscr{L}$ and the cut-off function Ξ. In addition, $\mathscr{W}^{(0)}$ is required to have a finite elastic energy.

https://doi.org/10.1017/S0956792501004703 Published online by Cambridge University Press

The discrepancy can be removed by setting appropriate boundary conditions for the functions $u_z^{(0)}$ and $u_\varphi^{(0)}$:

$$u_z^{(0)}|_{z=0} = \alpha_3, \quad u_\varphi^{(0)}|_{z=0} = \beta_3 R. \tag{A.10}$$

Furthermore, the analysis of the next term in the asymptotics of the junction layer gives

$$\begin{aligned}
&\mathscr{L}\Big(\frac{\partial}{\partial \boldsymbol{\xi}'}\Big)\mathscr{W}^{(1)}(\boldsymbol{\xi}') + [\mathscr{L}, \chi]\Big\{\mathscr{T}(\varepsilon\boldsymbol{\xi}') + \mathscr{R}(\mathbf{x}_0)\Big\} \\
&+[\mathscr{L}, \Xi]\Big\{\mathbf{u}^{(1)}\Big|_{z=0} + \xi_2 \frac{\partial \mathbf{u}^{(0)}}{\partial z}\Big|_{z=0}\Big\} = 0 \quad \text{in } G, \qquad (A.11) \\
&\boldsymbol{\Sigma}^{(\mathbf{n})}\Big(\frac{\partial}{\partial \boldsymbol{\xi}'}\Big)\mathscr{W}^{(1)}(\boldsymbol{\xi}') + [\boldsymbol{\Sigma}^{(\mathbf{n})}, \chi]\Big\{\mathscr{T}(\varepsilon\boldsymbol{\xi}') + \mathscr{R}(\mathbf{x}_0)\Big\} \\
&+[\boldsymbol{\Sigma}^{(\mathbf{n})}, \Xi]\Big\{\mathbf{u}^{(1)}\Big|_{z=0} + \xi_2 \frac{\partial \mathbf{u}^{(0)}}{\partial z}\Big|_{z=0}\Big\} = 0 \quad \text{on } \partial G. \qquad (A.12)
\end{aligned}$$

We require the principal force and moment vectors, associated with the load in (A.11), (A.12), to vanish. To satisfy this constraint we impose the following orthogonality conditions:

$$\begin{aligned}
&-\int_G \Big\{[\mathscr{L}, \chi]\Big(\mathscr{T}(\boldsymbol{\xi}', \log\varepsilon) + \mathscr{R}(\mathbf{x}_0)\Big) \\
&+[\mathscr{L}, \Xi]\Big(\mathbf{u}^{(1)}\Big|_{z=0} + \xi_2 \frac{\partial \mathbf{u}^{(0)}}{\partial z}\Big|_{z=0}\Big)\Big\} d\boldsymbol{\xi}' \\
&\int_{\partial G} \Big\{[\boldsymbol{\Sigma}^{(\mathbf{n})}, \chi]\Big(\mathscr{T}(\boldsymbol{\xi}', \log\varepsilon) + \mathscr{R}(\mathbf{x}_0)\Big) \\
&+[\boldsymbol{\Sigma}^{(\mathbf{n})}, \Xi]\Big(\mathbf{u}^{(1)}\Big|_{z=0} + \xi_2 \frac{\partial \mathbf{u}^{(0)}}{\partial z}\Big|_{z=0}\Big)\Big\} ds_{\boldsymbol{\xi}'} = 0, \qquad (A.13)
\end{aligned}$$

and

$$\begin{aligned}
&-\int_G \Big(-\xi_2\mathbf{e}^{(1)} + \xi_1\mathbf{e}^{(2)}\Big) \cdot \Big\{[\mathscr{L}, \chi]\Big(\mathscr{T}(\boldsymbol{\xi}', \log\varepsilon) + \mathscr{R}(\mathbf{x}_0)\Big) \\
&+[\mathscr{L}, \Xi]\Big(\mathbf{u}^{(1)}\Big|_{z=0} + \xi_2 \frac{\partial \mathbf{u}^{(0)}}{\partial z}\Big|_{z=0}\Big)\Big\} d\boldsymbol{\xi}' \\
&\int_{\partial G} \Big(-\xi_2\mathbf{e}^{(1)} + \xi_1\mathbf{e}^{(2)}\Big) \cdot \Big\{[\boldsymbol{\Sigma}^{(\mathbf{n})}, \chi]\Big(\mathscr{T}(\boldsymbol{\xi}', \log\varepsilon) + \mathscr{R}(\mathbf{x}_0)\Big) \\
&+[\boldsymbol{\Sigma}^{(\mathbf{n})}, \Xi]\Big(\mathbf{u}^{(1)}\Big|_{z=0} + \xi_2 \frac{\partial \mathbf{u}^{(0)}}{\partial z}\Big|_{z=0}\Big)\Big\} ds_{\boldsymbol{\xi}'} = 0. \qquad (A.14)
\end{aligned}$$

Direct use of (A.13), (A.14) yields the following representation for the force density along the junction contour Γ:

$$\mathbf{F} \cong F_z^{(0)}\mathbf{e}^{(z)} + F_\varphi^{(0)}\mathbf{e}^{(\varphi)}$$

where the components are determined by the formulae (compare with (4.9), (4.11)):

$$F_z^{(0)} = \frac{Eh}{1-\nu^2}\Big(\frac{\partial u_z^{(0)}}{\partial z} + \nu\frac{u_r^{(0)}}{R}\Big)\Big|_{z=0}, \tag{A.15}$$

and

$$F_\varphi^{(0)} = \frac{Eh}{2(1+\nu)}\frac{\partial u_\varphi^{(0)}}{\partial z}\Big|_{z=0}. \tag{A.16}$$

https://doi.org/10.1017/S0956792501004703 Published online by Cambridge University Press

We remark that the radial component F_r of the force and the local bending moments have the order $O(\varepsilon^3)$, and hence they are not required for the leading approximation.

Thus, we have employed the analysis of the boundary layer fields to derive the junction conditions (A.10) and the expressions for the reaction forces (A.15), (A.16).

Acknowledgements

A. G. Aslanyan would like to thank Liverpool University, Department of Mathematical Sciences, for the financial support and excellent academic environment.

References

[1] Aslanyan, A. G. & Lidskii, V. B. (1974) *Distribution of Eigenvalues of Thin Elastic Shells*. Nauka, Moscow.
[2] Aslanyan, A. G., Movchan, A. B. & Selsil, Ö. (2000) A universal asymptotic algorithm for elastic thin shells. *Euro. J. Appl. Math.* **11**, 573–594.
[3] Åslund, J. (1998) Asymptotic analysis of a mixed boundary value problem for the Laplacian in a 2D–3D multi-structure. Thesis No. 741, LIU-TEK-LIC-1998: 76, Linköping University.
[4] Berdichevski, V. L. (1983) *Variational Principles of Continuum Mechanics*. Nauka, Moscow.
[5] Ciarlet, P. G. (1997) *Mathematical Elasticity, Vol. II: Theory of plates*. North-Holland.
[6] Ciarlet, P. G. & Destuynder, P. (1979) A justification of the two-dimensional plate model. *J. Méc.* **18**, 315–344.
[7] Ciarlet, P. G. & Lods, V. (1996a) Asymptotic analysis of linearly elastic shells. Generalised membrane shells. *J. Elasticity*, **43**, 147–188.
[8] Ciarlet, P. G. & Lods, V. (1996b) Asymptotic analysis of linearly elastic shells. I. Justification of membrane shell equations. *Arch. Rational Mech. Anal.* **136**, 119–161.
[9] Ciarlet, P. G., Lods, V. & Miara, B. (1996) Asymptotic analysis of linearly elastic shells. II. Justification of flexural shell equations. *Arch. Rational Mech. Anal.* **136**, 163–190.
[10] Donnell, L. H. (1976) *Beams, Plates and Shells*. McGraw-Hill.
[11] Gol'denveizer, A. L., Lidskii, V. B. & Tovstik, P. E. (1979) *Free Vibrations of Thin Elastic Shells*. Nauka, Moscow.
[12] Kesavan, S. & Sabu, N. (2000) Two-dimensional approximation of eigenvalue problems in shell theory: flexural shells. *Chin. Ann. Math.* **21B**(1), 1–16.
[13] Kozlov, V. A., Maz'ya, V. G. & Movchan, A. B. (1994) Asymptotic analysis of a mixed boundary value problem in a multi-structure. *Asymptotic Analysis*, **8**, 105–143.
[14] Kozlov, V. A., Maz'ya, V. G. & Movchan, A. B. (1995) Asymptotic representation of elastic fields in a multi-structure. *Asymptotic Analysis*, **11**, 343–415.
[15] Kozlov, V. A., Maz'ya, V. G. & Movchan, A. B. (1996) Fields in nondegenerate 1D-3D elastic multi-structures. LiTH-MAT-R-96-14, Preprint, Linköping University.
[16] Kozlov, V. A., Maz'ya, V. G. & Movchan, A. B. (1999) *Asymptotic Analysis of Fields in Multi-structures*. Oxford University Press.

https://doi.org/10.1017/S0956792501004703 Published online by Cambridge University Press